Dynamic imaging of glacier structures at high-resolution using source localization: a dense seismic array experiment.

Ugo Nanni[1,*], Philippe Roux[2], Florent Gimbert[1] and Albanne Lecointre[2]

[1] IGE, Univ. Grenoble Alpes, CNRS, IRD, Grenoble, France

[2] ISTerre, Univ. Grenoble Alpes, Univ. Savoie Mont Blanc, CNRS, IRD, IFSTTAR, Grenoble, France

Corresponding author: Ugo Nanni (ugo.nanni0158@gmail.com)

[*]Now at Dept Geosciences, University of Oslo, Norway.

Key Points:

- We present an innovative array-processing approach to image glaciers structures through locating seismic sources with high-resolution.
- We investigate a large range of spatial phase coherences, from very low up to very high, over narrow frequency bands and short time windows.
- We image the spatial and temporal dynamics of sources originating from active and passive crevasses as well as from subglacial hydrology.

Abstract

Dense seismic array monitoring on glaciers combined with advanced array processing may help retrieve and locate a variety of seismic sources with unprecedented resolution and spatial coverage. Here we present an array methodology that goes beyond classical localization algorithms through gathering various types of sources (impulsive or continuous) into a single scheme and sort those by their associated array phase coherence. We demonstrate that we can retrieve the spatial and temporal dynamics of active crevasses with a metric resolution using sources with high phase coherence; the presence of diffracting materials (e.g. rocks) trapped in transverse crevasses using sources with moderate phase coherence; and the time evolution of two-dimensional maps of the subglacial water flow drainage system using sources with low phase coherence. With the ongoing increased use of dense seismic arrays, our study highlights the strength of using an appropriate seismological approach to image a wide range of subsurface structures.

Plain Language Summary

Over the past two decades, the growing use of dense seismic arrays has often overcome limitations of traditional observations methods and yielded new insights on the physics of subsurface process and properties. Yet scientific challenges remain to be addressed for using the appropriate array-processing approaches and automating the techniques on continuous data and in a multidimensional model space including 3D source locations and seismic wave velocity. In this paper we address such challenges in the particular case of monitoring glaciers,

which have the particularities to generate numerous sources of quite extraordinarily diverse nature, from impulsive to tremor like signals. We combine a physic-based and a statistical approach to explore the spatial coherency of the seismic field generated by such a diversity of sources. We show that even a partial spatial coherence remains rich in statistical information on concomitant and/or low amplitudes micro-seismic sources. This allows us to localize seismic sources at high-resolution (metric to decametric) and identify emerging patterns associated with a wide range of glacier features and their dynamics, ranging from active crevasses, debris in transverse passive crevasses and subglacial water flow. Such methodological and conceptual advance may enable a more efficient and complete imaging of geophysical objects.

1 Introduction

Over the past two decades, the use of dense seismic arrays has become widespread at all spatial scales in geophysics and seismology thanks to the development of low-cost autonomous and synchronized seismic sensors (Lin et al. 2013; Ben-Zion et al. 2015; Shen et al. 2012; Sergeant et al. 2020). On a continental scale, these networks of several hundred or thousands of sensors (e.g. USArray, Hi-Net (Ekström et al. 2009; Okada et al. 2004)) yielded accurate maps of phase and group velocities for surface waves in the frequency range where ocean-driven ambient seismic noise dominates (<~1 Hz). On a local scale (few to tens of kilometers), passive imaging and monitoring of the subsurface have become classical tools of geophysics with the investigation of higher frequency waves (few to tens of Hz) often generated by anthropogenic noise (Pinzon-Rincon et al. 2021). Seismic exploration conducted using active sources and a number of sensors often exceeding ten thousand has long been used for near-surface imaging purposes, particularly in the oil and gas industry (Lindseth 1968; Chmiel et al. 2021). With the growing monitoring capabilities now being affordable in academia, the scientific literature has recently been full of examples of the use of dense seismic networks on all kinds of geophysical objects and at all spatial scales, such as active faults, volcanoes, geothermal systems, landslides, glaciers, oil exploration fields. Thanks to the remote and non-invasive nature of seismic instrumentation, the use of dense seismic array often allows overcome limitations of traditional observation methods and yield new insights on the physics of subsurface process.

The use of dense seismic arrays requires array-processing techniques in which one analyzes the spatial coherence of the incident waves on all or part of the array, in accordance with the diffraction laws. Although very promising, the recent development of algorithms based on artificial intelligence and neural networks with or without learning stage (Bianco et al. 2019; Seydoux et al. 2020; Shi et al. 2021) does not yet take the place of wave physics as an essential tool to take advantage of the spatial density of sensor arrays (Seydoux et al. 2016). Current physics-based algorithms consist in evaluating the spatial coherence(s) between nearby sensors and on the whole network via the construction of the inter-spectral matrix (CSDM) at given frequencies (Cros et al. 2011). The measure

of the spatial coherence is then coupled to an inversion scheme (for imaging) or to a projection on a 2D/3D model space (for source localization), this last algorithm forming the fundamental principle of the widely used Matched Field Processing (MFP) (Vandemeulebrouck et al. 2013; Gresse et al. 2018). MFP algorithms lead to the interpretation of an "ambiguity surface" that represents the probability of the presence of a seismic source in the model space (Corciulo et al. 2012; Gradon et al. 2019; Gradon et al. 2021; Chmiel et al. 2019).

Applying MFP on massive data raises three main difficulties, which are (1) matching the appropriate surrogate source from the model space to the experimental data, (2) dealing with multiple and concomitant sources that degrades the spatial coherence of the CSDM and affects the quality of the projection of the propagation model, built on the basis of a point-like source or an incident plane wave, onto the data and (3) automating the technique on continuous and massive data and in a multidimensional model space including 3D source locations and phase velocity, for example.

In this paper, we address the above listed challenges in the specific case of the monitoring of glaciers, which have the particularities to generate numerous sources of quite extraordinarily diverse nature, from impulsive to tremor like signals (Podolskiy and Walter 2016). The aim of our study is to go beyond classical localization algorithms that generally assign a source to a time window for high phase coherencies, and that reject time windows where the phase coherence is low and localization is ambiguous. We combine an efficient MFP algorithm and a statistical approach in order to gather all the diversity of sources into a single scheme. We show that, despite the ambiguity on localization, a partial coherence on the array remains rich in statistical information on concomitant and/or low amplitudes micro-seismic sources. Sorting all sources by degree of phase coherence, we identify distinct patterns associated with different glacier features and their dynamics, ranging from active crevasses, debris in transverse crevasses and subglacial water flow.

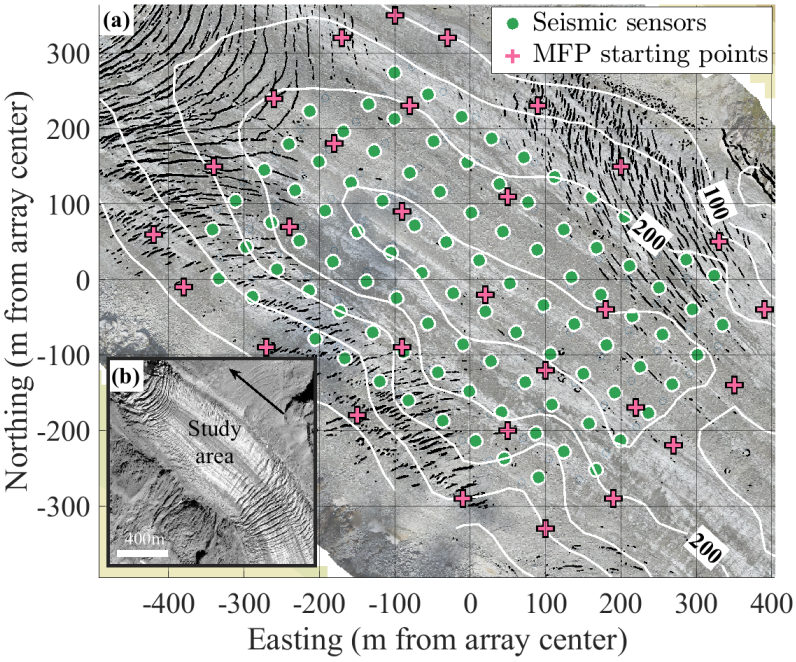

Fig. 1: (a) Monitoring set-up of Glacier d'Argentière and (b) aerial view of the Glacier d'Argentière field site (France, Mont Blanc mountain range). (a) The seismic network (green dots) is composed of 98 seismic stations with Fairfield Nodal Z-Land 3 components, which are indicated according to their positions at the beginning of the survey period. White contour lines show 50-m-spaced ice thickness contours, as obtained from combined radar measurements and surface elevations. The pink crosses show the locations of the 29 starting points used in the location algorithm. The glacier flows toward the northwest (top left) as shown by the black arrow in (b). Aerial view provided by Bruno Jourdain.

2 Materials and Methods

2.1 Field experiment

Our study lies in the context of the RESOLVE project (Gimbert et al. 2021), which consisted in the deployment of 98 seismic sensors on the Argentière Glacier in the French Alps (Fig. 1). The network covered an area of about 650m x 800m in the lower part of the glacier, with a station interspacing of about 40 m. Continuous acquisition were made during 35 days at the onset of the 2018's melt season (April-June). This area is also well documented through other local measurements (Gimbert et al. 2021). Based on this complementary information we know that the glacial surface velocity was on the order of 0.1 m.day^{-1} during the dense array campaign and that subglacial water discharge increased from 0.1 m^3.sec^{-1} on April 24th to 4 m^3.sec^{-1} on May 30th. Geophysical imaging through ambient seismic noise correlation has already been conducted with this seismic

dataset as well as the identification of coherent seismic sources (icequake) located on the surface (crevasses, block falls) and at the rock-glacier interface (Sergeant et al. 2020). At high frequencies [10-20] Hz, short and repeated pulses that cross the entire network dominate the seismic signal with a few seconds recurrence time (Gimbert et al. 2021). This very large population of icequakes is mostly composed of surface waves (phase velocity = 1590 m/s). At low frequency [3-7] Hz, subglacial water flow has been observed to generate continuous seismic noise (Nanni et al. 2020) and a dynamic mapping of hydrological flows at the base of the glacier was carried out via the study of incoherent and spatially dispersed seismic sources (Nanni et al. 2021).

2.2 Data analysis

We focus on ground motion extracted from the vertical component of the nodes. We conduct MFP by recursively matching a synthetic field of phase delays between sensors with that obtained from observations using the Fourier transform of time-windowed data. We obtain the synthetic field from a source model with a frequency-domain Green's function that depends on source spatial coordinates x, y and z and medium phase velocity c. We use a spatially homogeneous velocity field within the glacier, which has the advantage of a fast-analytical computation, although it also results in a higher degree of ambiguity between z and c. To build a large catalog of events, we apply MFP over the entire study period using short time windows of T=1 s with 0.5-s overlap, across frequency bands of $\pm$2 Hz width evenly spaced from 5 to 20 Hz. Our approach considers spherical waves and allows locating point-like sources close to and even within the seismic array (Gimbert et al. 2021). In order to preserve a quality of source localization we keep only the sources detected within the glacier at less than 400 m from the center of the seismic network and with realistic phase velocities within [1000-3500] m.sec^{-1} (Sergeant et al. 2020; Nanni et al. 2021). We limit our spatial analysis on the glacier's surface plane because of (1) the depth-vs-velocity ambiguity of the MFP due to the 2D disposition of our array and (2) the large spreading of the surface wave sensivity kernel with depth (Gimbert et al. 2021).

At each frequency, the MFP output is a marker of the spatial coherence among the array (Vandemeulebrouck et al. 2013). It ranges from 0 to 1 with higher values corresponding to better matches between modelled and observed signal phases, which is classically interpreted as a higher confidence in true source location (Cros et al. 2011; Gresse et al. 2018; Corciulo et al. 2012; Gradon et al. 2019; Gradon et al. 2021). One should note, however, that across frequencies, a source located with a similar MFP output does not bear the same accuracy, since the spatial phase coherence increases with increasing seismic wavelength (Rost and Thomas 2002). For instance, a partial coherence on 5 to 10 neighboring sensors (with inter-distance of about 40 m) would lead to a MFP output around 0.05 at high frequencies of about 20 Hz (seismic wavelength of about 80 m) while around 0.1 at frequencies of about 10 Hz (seismic wavelength of about 160 m).

It can occur that within a given time window T simultaneous micro-seismic sources of varying amplitudes occur, which causes wavefield superposition and a drop in the spatial coherence. As a result, a large number of local minima characterize the exploration of the model space at each frequency. In order to properly probe local minima (Gradon et al. 2021; Chmiel et al. 2019), we start the minimization algorithm from a set of 29 points widely distributed inside and near the array at the glacier surface (pink crosses in Fig. 1). The originality of our approach is to keep all MFP outputs of the 29 minimizations found after convergence and analyze these statistical results through the distribution of MFP values. Such an approach is made possible through drastically reducing computational cost using an algorithm that relies on the downhill simplex search method (Nelder-Mead optimization) (Lagarias et al. 1999) instead of using a multi-dimensional grid search approach.

Two extreme cases give an idea of the population of localizations obtained by our MFP algorithm. When a single icequake signal is present in the study window T, the 29 minimizations are expected to converge to a single source location with an MFP level close to 1 (Sergeant et al. 2020; Gimbert et al. 2021). On the contrary, if the time window T records only random noise, the 29 minimizations are expected to generate as many localizations scattered over the whole study area with an MFP level of the order of $1/N$ where $N = 98$ is the total number of sensors in the seismic array. Between these two extremes, the case of multiple sources leads to clusters of localizations.

Through the diversity of sources encountered within a glacier, the results presented below scan the different degree of spatial phase coherence obtained by MFP minimization initialized from different starting points and show the strategies to be developed to image at high-resolution a variety of glacier structures with source localization techniques.

3 Results

3.1 Imaging crevasse dynamics from impulsive events

In Figure 2a, we show the spatial distribution of the seismic events associated with a high (i.e. global) phase coherence (MFP output, [0.5-1]; frequency, [15-19] Hz). For these events, the convergence of the location algorithm leans towards the global minimum of the cost function, whatever the starting point of the minimization (Gimbert et al. 2021). We observe that the events are mainly located on the side of the glaciers where crevasses are observed (Figs. 1a, 2a) and have a relatively low occurrence of c. 1 event per day per square meter. On the eastern and western flanks of the glacier where ice is thinner, the events are almost aligned orthogonally to the glacier flow, whereas on the northern part of our study area, they tend to align along flow. Such pattern is typically expected for crevasses of narrow U-shaped valley glacier as a result of maximum extensive stresses rotating form near along flow to near perpendicular flow due to increased shearing as approaching the glacier sides (Colgan et al. 2016). In Figure 2b, we show the temporal dynamics of the events observed on April 25^{th}

between 0:00 and 10:00 am UTC and located within the seismic array. Over the course of the day, the crevasses activation migrates at a speed of c. 10 m.s^{-1}, allowing us to draw the complete geometry of the c. 150 m-long crevasses buried under about 4 meters of snow. On the eastern part of the crevasse, where the spatial spreading of the events is relatively large (c. 50m), no large crevasses are observed on the surface (Figs. 1a, 2b) suggesting more diffuse and smaller structures than on the western side where clear localized structures are visible on the surface. In this later area, the geometry depicted by the successive events presents a narrow width of about or less than ten meters, which is considerably lower than the half-wavelength (c. 45 m for a 17 Hz central frequency, Fig. 2c). It thus appears that our localization accuracy is better than expected based on the classical limits of wave diffraction defined in the far field (i.e. for source-to-stations distances greater than the wavelength) (Fink et al. 2000). This is further evidenced in Figure 2c, where we observe that the focal spot obtained from matched field processing on a grid search conducted for the event identified with the green cross (Fig. 2b, c) has a width of about 100 m, which is much larger than the apparent resolution of about ten meters depicted by the events alignment along the crevasse. This show that keeping only the centre of the focal spot as shown in Fig. 2c, leads to ultra-high resolution imaging of dynamical structures, in a similar way to what is done in optics (Betzig et al. 2006; Rust et al. 2006). This also leads us to advance that the spread of sources on the eastern side of the crevasse is real and not due to localization uncertainties.

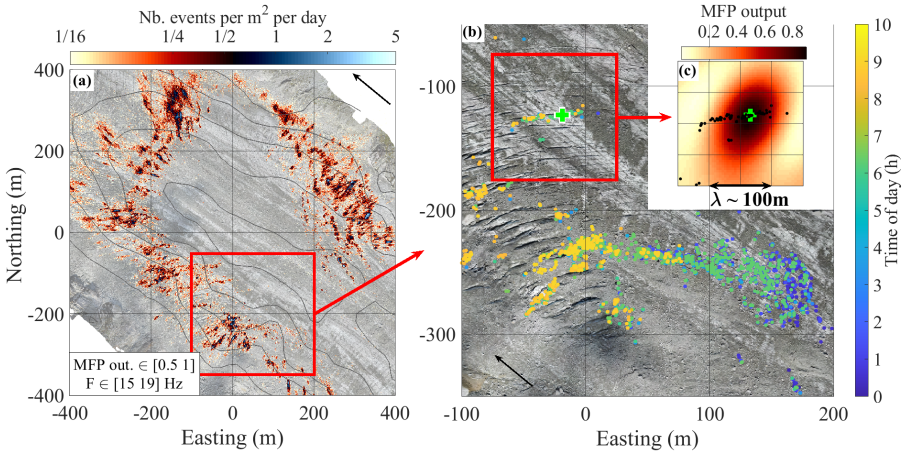

Fig. 2: Two-dimensional maps of source location obtained from matched-field processing (MFP) for the 17 ±2 Hz frequency range and the [0.5-1] MFP output range. (a) Map averaged over a 30-day time windows. The color scale shows the number of events per square meter per day. Contour lines show the 50-m-spaced ice thickness contours, as shown in Figure 1a. Red square shows zoom of panel (b). Black arrow shows glacier flow direction. (b) Source location obtained for April 25$^{\text{th}}$ between 0:00 and 10:00 am UTC. The color scale shows the time of each event. Red square shows zoom of panel (c). (c) Diffraction-based spatial

focus obtained from MFP for the event identified with the green cross. The color scale shows the MFP output values. Black dots show localized seismic sources.

3.2 Imaging sub-surface structures from diffracted waves

In Figure 3a, we show the spatial distribution of the seismic events associated with an intermediate (local) phase coherence (MFP output, [0.07-0.16]; frequency, [11-15] Hz). With these intermediate phase coherencies, the data versus model phase agreement is only local and all 29 localizations obtained from the minimization algorithm are expected to be spatially dispersed. We observe that, when averaged over multiple days, the spatial distribution of the events draws clear structures that are transverse to the glacier flow and are particularly marked in the upstream and downstream parts of the seismic network (Fig. 3a). These structures are regularly spaced by c. 50 m, and 8 of them have an average event density of around 10 per day per square meter, which is significantly higher than previously found for crevasse sources at high coherency (Sect. 3.1). The typical width of the transverse structures (c. 10m) remains significantly lower than the half-wavelength (c. 60 m for a 13 Hz central frequency) thus further supporting our previous finding that location precision is higher than the typical half-wavelength. In Fig. 3b, we show with more details the downstream part of our seismic array where three lines of events are well distinguishable, to be compared with Fig. 3c where we show a picture of the same area taken from helicopter. In this picture, we identify 3 to 4 across-flow transverse crevasses with a geometry similar to that of the lines of events identified with seismic. Such transverse crevasses are thought to be inherited from large crevasses formed upstream (see Fig. 1b) and having progressively closed as advected downstream under a more compressive stress environment (Colgan et al. 2016). Despite being small and likely inactive, we suggest that these relict crevasses create a sufficiently strong material contrast for diffraction to occur and our algorithm to detect diffractions as "events". Such a strong material contrast is likely permitted by the presence of rock debris having entered these relict crevasses when those were previously active and large. Analysis of lower spatial phase coherencies in the MFP algorithm can therefore allow identifying diffractors, which would not have been permitted in a classical MFP framework since each of these localizations would have been ignored based on their low spatial coherence. This shows the strong potential of our statistical analysis, which highlights the meaning of retrieving event locations in an attempt to not only study true seismic sources but also scattering structures (Fig. 3b,c).

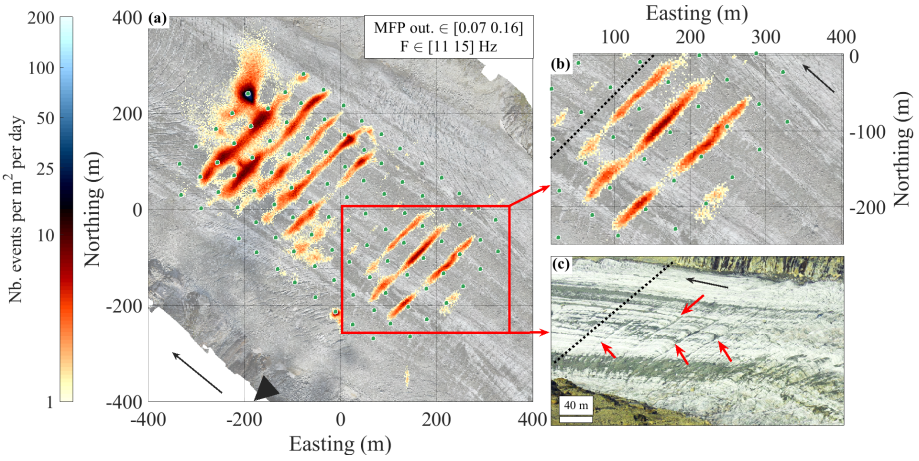

Fig. 3: (a) Two-dimensional maps of the source location densities obtained for the 13 ± 2 Hz frequency range and the [0.07-0.16] MFP output range averaged over a 30-day time windows. The color scale shows the number of events per square meter per day. Black arrow shows glacier flow direction. (b) Zoom on the downglacier part of our array. Black dotted-line is orthogonal to glacier flow. (c) Helicopter view of the study area from the right flank of the Glacier d'Argentière. Line of sight is shown in (a) with the black triangle. Red arrows show crevasses traces at the surface of the glacier. Black dotted-line is the same as in (b). Aerial view provided from Bruno Jourdain, September 2018.

3.3 Imaging the subglacial hydrology dynamics from incoherent noise

In Figure 4, we show the spatial and temporal distribution of the seismic events associated with the lowest (i.e. local) phase coherence (MFP output, [0.07-0.16]; frequency, [3-7] Hz). The localizations shown in Fig. 4 are expected to be more dispersed and less reliable than in Fig. 3a, because of the larger wavelengths and therefore a lower phase coherence. By considering sources over the whole period we observe a characteristic pattern of sources aligning along the glacier centerline, where the ice is at maximum thickness and where hydraulic potential calculations (Fig. 4a) suggest the likely location of subglacial water flow (Nanni et al. 2021). These sources are studied in details in Nanni et al. (2021), who showed that they are likely generated at depth near the glacier bed and are associated with subglacial hydrology flows. At such low frequencies, the localization resolution is expected to be limited to 50 to 150 m (i.e. 1/6 to 1/2 of the c. 300 m wavelength). The width of the observed spot (c. 50 m) is likely due to this reduced localization resolution as a result of the limited number of sensors being sensitive to a given source, although we cannot rule out that it could also be due to sources being distributed.

The temporal evolution observed from Fig. 4a to Fig. 4d highlights a significant increase of source density from around 1 event per day per square meter up to 15 events per day per square meter over the one month of instrumentation,

consistent with subglacial flow discharge and the associated generated seismic noise strongly increasing over the period (Nanni et al. 2020). This evolution is associated with a transition from a distributed to a more localized pattern, which was identified by Nanni et al. (2021) as the signature of the subglacial hydrology dynamics in response to an increase in surface melt, consistent with expectations based on numerous glacier observational and numerical studies in different contexts (Tranter et al. 1996; Lewington et al. 2020; Davison et al. 2019; Vincent and Moreau 2016; Irarrazaval et al. 2021). Despite the very low phase coherence at such MFP output range, we thus observe coherent pattern of sources with a temporal dynamic that is significant enough to be used to study and image the subglacial hydrology networks.

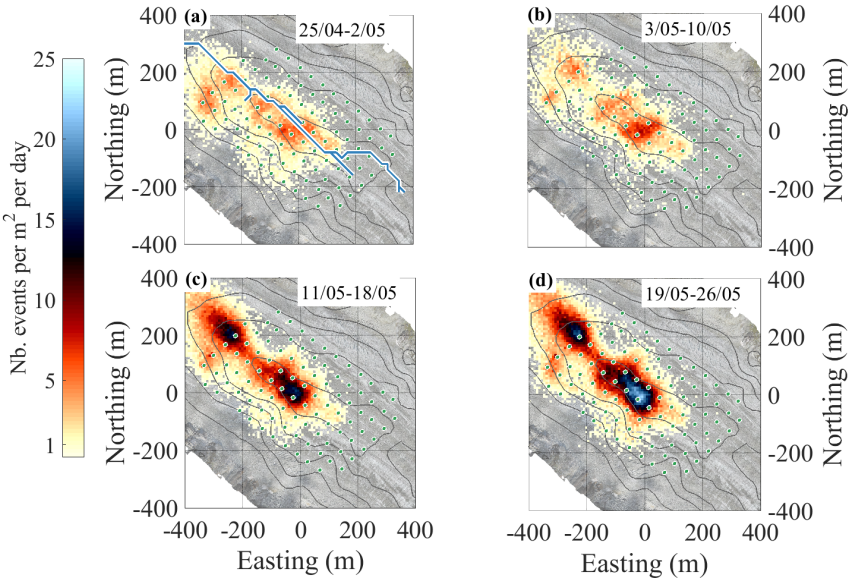

Fig. 4: (a to d) Temporal evolution of the spatial patterns of the source location densities obtained for the 5 ±2 Hz frequency range and the [0.07-0.16] MFP output range. All of the maps are averaged over 7-day time windows. Color scale shows the number of events per square meter per day. Contour lines show the 50-m-spaced ice thickness contours, as shown in Figure 1. The blue line in (a) shows the path that minimizes the hydraulic potential gradient calculated with a flotation fraction of 0.5 in Nanni et al. (2021), which represents the likely location of subglacial waterways.

4 Discussion and Conclusions

4.1 Source location accuracy

We observe that the horizontal resolution at which we retrieve sources with our MFP scheme, whether they are generated by actives/inactive crevasses (Figs. 2, 3) or by subglacial water flow (Fig. 4), is of about 1/6 to 1/12 of the investigated wavelength. Such a resolution is much higher than expected under a far

field investigation, which is considered to be limited to half of the investigated wavelength (Fink et al. 2000). We suggest that the high resolution obtained in our case is made possible thanks to our array disposition that allows subwavelength sampling and cover all azimuthal directions around the targeted sources (Rost and Thomas 2002) and by our focus on sources within and close to the array, resulting in a near-field investigation of the wavefield, which is considered to yield a resolution down to 1/8 of the investigated wavelength (Pyrak-nolte et al. 1999).

For the highest coherence values (Fig. 2), we obtain a hyper-resolved imaging of active and superficial crevasses in all respects similar to that observed in super-resolved optical imaging (Hess et al. 2006). This allows us to draw with details the geometry of a crevasse that is revealed accurately by the repetition of nearby micro-icequakes in active crevasses through our statistical approach. With our resolution we do not simply image the most localized parts of crevasses but also locations where those are more diffuse. Such approach may yield key observations for the study of the mechanisms controlling the propagation of crevasses, which is a topic of important matter for the dynamics of the Greenland Ice sheet (Roeoesli et al. 2016) and the Antarctic Ice shelfs (MacAyeal et al. 2019).

For the lowest coherence values (Figs. 3, 4) we also obtain highly-resolved images of subsurface transverse crevasses, with a c. 10 m resolution, and subglacial hydrology networks, with a c. 50 m resolution. Traditionally, events located with such low phase coherence are discarded because considered of low confidence. However, by summing these localizations over time, we obtain reliable observation of glaciers structures and their dynamics. This shows the advantage of applying a statistical approach downstream of a fine localization of a very large number of sources over time.

4.2 Advances and perspectives in the investigation of phase coherence

The repetition and multiplication of impulse seismic sources of the icequake type, but also the superposition with ambient noise of a hydraulic nature, requires a more complete physical and statistical study of the recorded signal that what is traditionally done. In practice, it appears that each time window T (~1s) contains spatially correlated information on all or part of the seismic network. Extracting this spatial coherence requires then (1) not to be limited to the strong MFP values classically used to confirm the detection of a microseismic source, (2) to allow MFP analysis by narrow frequency bands (~+/- 2Hz) for seismic wavelengths well sampled by the network and (3) to let the MFP algorithm explore the parameter space in search of local minima via a gradient descent technique initiated at different points inside and outside the seismic network. The novelty of the observations yielded from our MFP investigation lies also on the diversity of the observed sources, compared to previous studies that used a similar methodological approach (Gradon et al. 2021; Chmiel et al. 2019). We observe (1) impulsive events with clear arrival time and high phase coherence, (2) incoherent seismic noise generated from water turbulences and (3) diffracting

objects that, to our knowledge, have not been observed before with seismic a source localization scheme.

The wealth of information extracted from such a complete MFP analysis is promising for the understanding of the physical processes at play in complex systems hosting a large diversity of processes that generate numerous sources, from impulsive to tremor like signals, such as glaciers, active volcanoes, landslides or active fault zones. In a time of increasing use of dense seismic arrays, our study highlights how an accurate physic-based approach can be used to image with high accuracy sub-structures through a high-resolution localization of a variety of seismic sources. It also highlights the potential to apply a statistical and/or deep learning approach downstream of a physic-based approach to enhance the level of comprehension on large seismic dataset.

Acknowledgments

The authors declare no financial conflict of interest. This work has been conducted in the framework of the RESOLVE Project (https://resolve.osug.fr/) (LabEx OSUG@2020, Investissement d'avenir – ANR10LABX56 and IDEX Université Grenoble Alpes). Most of the computations presented in this paper were performed using the GRICAD infrastructure (https://gricad.univ-grenoble-alpes.fr), which is supported by Grenoble research communities, and with the CiGri tool (https://github.com/oar-team/cigri) that was developed by Gricad, Grid5000 (https://www.grid5000.fr) and LIG (https://www.liglab.fr/). FG acknowledges support from ANR SEISMORIV (ANR-17-CE01-0008) and SAUSSURE (ANR-18-CE01-0015-01).

Data

The data associated with the dense array experiment, including the actives crevasses investigation (Sect. 3.1), are available via https://doi.org/10.5281/zenodo.3971815 under a creative commons attribution 4.0 international license (Gimbert et al. 2021). The data associated with the transverse crevasses investigation (Sect. 3.2) are available via https://doi.org/10.5281/zenodo.5416435 under a creative commons attribution 4.0 international license. The data associated with the subglacial hydrology investigation (Sect. 3.3) are available via https://doi.org/10.5281/zenodo.3971815 under a creative commons attribution 4.0 international license (Nanni et al. 2021).

References

Ben-Zion, Yehuda, Frank L. Vernon, Yaman Ozakin, Dimitri Zigone, Zachary E. Ross, Haoran Meng, Malcolm White, Juan Reyes, Dan Hollis, and Mitchell Barklage. 2015. "Basic Data Features and Results from a Spatially Dense Seismic Array on the San Jacinto Fault Zone." *Geophysical Journal International* 202 (1): 1–11. https://doi.org/10.1093/gji/ggv142.Betzig, Eric, George H Patterson, Rachid Sougrat, O Wolf Lindwasser, Scott Olenych, Juan S Bonifacino, Michael W Davidson, Jennifer Lippincott-Schwartz, and Harald F Hess. 2006. "Imaging Intracellular Fluorescent Proteins at Nanometer Resolution."

Science 313 (5793): 1642–45.Bianco, Michael J, Peter Gerstoft, James Traer, Emma Ozanich, Marie A Roch, Sharon Gannot, and Charles-Alban Deledalle. 2019. "Machine Learning in Acoustics: Theory and Applications." *The Journal of the Acoustical Society of America* 146 (5): 3590–3628.Chmiel, Małgorzata, Philippe Roux, and Thomas Bardainne. 2019. "High-Sensitivity Microseismic Monitoring: Automatic Detection and Localization of Subsurface Noise Sources Using Matched-Field Processing and Dense Patch Arrays." *Geophysics* 84 (6): KS211–23. https://doi.org/10.1190/geo2018-0537.1.Chmiel, Małgorzata, Philippe Roux, Marc Wathelet, and Thomas Bardainne. 2021. "Phase-Velocity Inversion from Data-Based Diffraction Kernels: Seismic Michelson Interferometer." *Geophysical Journal International* 224 (2): 1287–1300.Colgan, William, Harihar Rajaram, Waleed Abdalati, Cheryl McCutchan, Ruth Mottram, Mahsa S. Moussavi, and Shane Grigsby. 2016. "Glacier Crevasses: Observations, Models, and Mass Balance Implications." *Reviews of Geophysics* 54 (1): 119–61. https://doi.org/10.1002/2015RG000504.Corciulo, Margherita, Philippe Roux, Michel Campillo, Dominique Dubucq, and W A Kuperman. 2012. "Multiscale Matched-Field Processing for Noise-Source Localization in Exploration Geophysics." *Geophysics* 77 (5).Cros, E., P. Roux, J. Vandemeulebrouck, and S. Kedar. 2011. "Locating Hydrothermal Acoustic Sources at Old Faithful Geyser Using Matched Field Processing." *Geophysical Journal International* 187 (1): 385–93. https://doi.org/10.1111/j.1365-246X.2011.05147.x.Davison, Benjamin Joseph, Andrew John Sole, Stephen John Livingstone, Tom R. Cowton, and Peter William Nienow. 2019. "The Influence of Hydrology on the Dynamics of Land-Terminating Sectors of the Greenland Ice Sheet." *Frontiers in Earth Science* 7. https://doi.org/10.3389/feart.2019.00010.Ekström, Göran, Geoffrey A. Abers, and Spahr C. Webb. 2009. "Determination of Surface-Wave Phase Velocities across USArray from Noise and Aki's Spectral Formulation." *Geophysical Research Letters* 36 (18): 5–9. https://doi.org/10.1029/2009GL039131.Fink, Mathias, Didier Cassereau, Arnaud Derode, Claire Prada, Philippe Roux, Mickael Tanter, Jean-Louis Thomas, and François Wu. 2000. "Time-Reversed Acoustics." *Reports on Progress in Physics* 63 (12): 1933.Gimbert, Florent, Ugo Nanni, Philippe Roux, Agnès Helmstetter, Stéphane Garambois, Albanne Lecointre, Andréa Walpersdorf, et al. 2021. "A Multi-Physics Experiment with a Temporary Dense Seismic Array on the Argentière Glacier, French Alps: The RESOLVE Project." *Seismological Research Letters*, February. https://doi.org/10.1785/0220200280.Gradon, Chloe, Ludovic Moreau, Philippe Roux, and Yehuda Ben-Zion. 2019. "Analysis of Surface and Seismic Sources in Dense Array Data with Match Field Processing and Markov Chain Monte Carlo Sampling." *Geophysical Journal International* 218 (2): 1044–56. https://doi.org/10.1093/gji/ggz224.Gradon, Chloé, Philippe Roux, Ludovic Moreau, Albanne Lecointre, and Yehuda Ben Zion. 2021. "Characterization with Dense Array Data of Seismic Sources in the Shallow Part of the San Jacinto Fault Zone." *Geophysical Journal International* 224 (2): 1133–40.Gresse, Marceau, Jean Vandemeulebrouck, Svetlana Byrdina, Giovanni Chiodini, Philippe Roux, Antonio Pio Rinaldi, Marc Wathelet, et al. 2018. "Anatomy of a Fumarolic System Inferred from a Multiphysics Approach." *Scientific*

Reports 8 (1): 1–11.Hess, Samuel T, Thanu P K Girirajan, and Michael D Mason. 2006. "Ultra-High Resolution Imaging by Fluorescence Photoactivation Localization Microscopy." *Biophysical Journal* 91 (11): 4258–72.Irarrazaval, Inigo, Mauro A Werder, Matthias Huss, Frederic Herman, and Gregoire Mariethoz. 2021. "Determining the Evolution of an Alpine Glacier Drainage System by Solving Inverse Problems." *Journal of Glaciology* 67 (263): 421–34. https://doi.org/10.1017/jog.2020.116.Lagarias, J C, J A Reeds, M H Wright, and P E Wright. 1999. "Convergence Behavior of the Nelder-Mead Simplex Algorithm in Low Dimensions." *SIAM J. Optimization* 9: 112–47.Lewington, Emma L. M., Stephen J. Livingstone, Chris D. Clark, Andrew J. Sole, and Robert D. Storrar. 2020. "A Model for Interaction between Conduits and Surrounding Hydraulically Connected Distributed Drainage Based on Geomorphological Evidence from Keewatin, Canada." *The Cryosphere* 14 (9): 2949–76. https://doi.org/10.5194/tc-14-2949-2020.Lin, Fan-Chi, Dunzhu Li, Robert W Clayton, and Dan Hollis. 2013. "High-Resolution 3D Shallow Crustal Structure in Long Beach, California: Application of Ambient Noise Tomography on a Dense Seismic ArrayNoise Tomography with a Dense Array." *Geophysics* 78 (4): Q45--Q56.Lindseth, Roy O. 1968. "Seismic Data Inversion." In *Digital Processing of Geophysical Data-A Review*, 11–12. Society of Exploration Geophysicists.Macayeal, Douglas R, Alison F Banwell, Emile A Okal, Jinqiao Lin, Ian C Willis, Becky Goodsell, and Grant J Macdonald. 2019. "Diurnal Seismicity Cycle Linked to Subsurface Melting on an Ice Shelf." *Annals of Glaciology* 60 (79): 137–57. https://doi.org/10.1017/aog.2018.29.Nanni, Ugo, Florent Gimbert, Philippe Roux, and Albanne Lecointre. 2021. "Observing the Subglacial Hydrology Network and Its Dynamics with a Dense Seismic Array." *Proceedings of the National Academy of Sciences* 118 (28). https://doi.org/https://doi.org/10.1073/pnas.2023757118.Nanni, Ugo, Florent Gimbert, Christian Vincent, Dominik Gräff, Fabian Walter, Luc Piard, and Luc Moreau. 2020. "Quantification of Seasonal and Diurnal Dynamics of Subglacial Channels Using Seismic Observations on an Alpine Glacier." *Cryosphere* 14 (5): 1475–96. https://doi.org/10.5194/tc-14-1475-2020.Okada, Y., K. Kasahara, H. Sadaki, and K. Obara. 2004. "Recent Progress of Seismic Observation Networks in Japan." *Earth Planets Space* 56 (1). https://doi.org/10.1088/1742-6596/433/1/012039.Pinzon-Rincon, Laura, François Lavoué, Aurélien Mordret, Pierre Boué, Florent Brenguier, Philippe Dales, Yehuda Ben-Zion, Frank Vernon, Christopher J Bean, and Daniel Hollis. 2021. "Humming Trains in Seismology: An Opportune Source for Probing the Shallow Crust." *Seismological Society of America* 92 (2A): 623–35.Podolskiy, Evgeny A., and Fabian Walter. 2016. "Cryoseismology." *Reviews of Geophysics* 54 (4): 708–58. https://doi.org/10.1002/2016RG000526.Pyraknolte, Laura J, Beth L Mullenbach, Xun Li, David D Nolte, and Abraham S Grader. 1999. "Synthetic Sediments Using Seismic Wave Transmission Sample." *Geophysical Research Letters* 26 (1): 127–30.Roeoesli, Claudia, Agnes Helmstetter, Fabian Walter, and Edi Kissling. 2016. "Meltwater Influences on Deep Stick-Slip Icequakes near the Base of the Greenland Ice Sheet." *Journal of Geophysical Research F: Earth Surface* 121 (2): 223–

40. https://doi.org/10.1002/2015JF003601.Rost, Sebastian, and Christine Thomas. 2002. “Array Seismology: Methods and Applications.” *Reviews of Geophysics* 40 (3): 2-1-2–27. https://doi.org/10.1029/2000RG000100.Rust, Michael J, Mark Bates, and Xiaowei Zhuang. 2006. “Sub-Diffraction-Limit Imaging by Stochastic Optical Reconstruction Microscopy (STORM).” *Nature Methods* 3 (10): 793–96.Sergeant, Amandine, Malgorzata Chmiel, Fabian Lindner, Fabian Walter, Philippe Roux, Julien Chaput, Florent Gimbert, and Aurelien Mordret. 2020. “On the Green’s Function Emergence from Interferometry of Seismic Wave Fields Generated in High-Melt Glaciers: Implications for Passive Imaging and Monitoring.” *Cryosphere* 14 (3): 1139–71. https://doi.org/10.5194/tc-14-1139-2020.Seydoux, L, N M Shapiro, J. de Rosny, and M Landès. 2016. “Spatial Coherence of the Seismic Wavefield Continuously Recorded by the USArray.” *Geophysical Research Letters* 43 (18): 9644–52. https://doi.org/10.1002/2016GL070320.Seydoux, Léonard, Randall Balestriero, Piero Poli, Maarten De Hoop, Michel Campillo, and Richard Baraniuk. 2020. “Clustering Earthquake Signals and Background Noises in Continuous Seismic Data with Unsupervised Deep Learning.” *Nature Communications* 11 (1): 1–12.Shen, Yang, Yong Ren, Haiying Gao, Brian Savage, R. G. Stockwell, Laurent Stehly, Paul Cupillard, et al. 2012. “Journal of Geophysical Research : Solid Earth Body Wave Extraction and Tomography at Long Beach , California , with Ambient-Noise Interferometry.” *Geophysical Journal International* 120 (8–9): 1159–73. https://doi.org/10.1002/2015JB011870.Received.Shi, Peidong, Léonard Seydoux, and Piero Poli. 2021. “Unsupervised Learning of Seismic Wavefield Features: Clustering Continuous Array Seismic Data During the 2009 L’Aquila Earthquake.” *Journal of Geophysical Research: Solid Earth* 126 (1): e2020JB020506. https://doi.org/10.1029/2020JB020506.Tranter, Martyn, Giles H Brown, Andrew J Hodson, and Angela M Gurnell. 1996. “Hydrochemistry as an Indicator of Subglacial Drainage System Structure: A Comparison of Alpine and Sub-Polar Environments.” *Hydrological Processes* 10 (4): 541–556. https://doi.org/10.1002/(SICI)1099-1085(199604)10:4<541::AID-HYP391>3.3.CO;2-0.Vandemeulebrouck, J., P. Roux, and E. Cros. 2013. “The Plumbing of Old Faithful Geyser Revealed by Hydrothermal Tremor.” *Geophysical Research Letters* 40 (10): 1989–93. https://doi.org/10.1002/grl.50422.Vincent, Christian, and Luc Moreau. 2016. “Sliding Velocity Fluctuations and Subglacial Hydrology over the Last Two Decades on Argentière Glacier, Mont Blanc Area.” *Journal of Glaciology* 62 (235): 805–15. https://doi.org/10.1017/jog.2016.35.